Eulerian - Eulerian Large Eddy Simulations Applied to Non-Reactive Transient Diesel Sprays.

Anthony Robert, Lionel Martinez, Julien Tillou, Stéphane Richard

IFP Energies nouvelles International Conference
Rencontres Scientifiques d'IFP Energies nouvelles

LES4ICE 2012 - Large Eddy Simulation for Internal Combustion Engine Flows
LES4ICE 2012 - La simulation aux grandes échelles pour les écoulements dans les moteurs à combustion interne

Eulerian – Eulerian Large Eddy Simulations Applied to Non-Reactive Transient Diesel Sprays

Anthony Robert, Lionel Martinez, Julien Tillou and Stéphane Richard*

IFP Energies nouvelles, 1-4 avenue de Bois-Préau, 92852 Rueil-Malmaison - France
e-mail: stephane.richard@ifpen.fr

* Corresponding author

Résumé — **Évaluation de la méthode Euler – Euler pour la simulation aux grandes échelles de sprays Diesel instationnaires non-réactifs** — L'objectif de cette étude est de réaliser et d'analyser des simulations aux grandes échelles (LES, Large Eddy Simulations) de sprays Diesel instationnaires dans une cellule haute pression et haute température. Pour représenter les stratégies d'injection d'un moteur Diesel actuel, deux cas sont analysés : le premier est une mono-injection, et une double injection est ensuite simulée. Pour chaque configuration, plusieurs réalisations sont calculées pour obtenir les valeurs moyennes et les fluctuations de concentration en carburant. Une sensibilité au maillage est réalisée pour juger de la qualité du maillage en comparant les profils numériques de fraction massique de carburant aux profils expérimentaux. Cette comparaison est également étendue aux pénétrations vapeur et aux angles de sprays. Ensuite, l'influence sur les résultats numériques de la condition limite d'injection, du profil de taux d'introduction, ainsi que du retard à l'injection sont évalués. Pour finir, des recommandations pour les futures simulations LES de sprays instationnaires en moteur Diesel sont suggérées.

Abstract — *Eulerian – Eulerian Large Eddy Simulations Applied to Non-Reactive Transient Diesel Sprays* — *The aim of this study is to perform and analyze LES (Large Eddy Simulations) simulations of transient Diesel sprays in a high-pressure and high-temperature vessel. In order to be representative of real Diesel injection strategies, two cases are investigated: the first one corresponds to a single injection, while a double injection is performed in the second case. For each case, numerous realizations are computed to retrieve average values and fluctuations of fuel concentration. A mesh refinement sensitivity analysis is conducted to assess the quality of the LES by comparing numerical fuel mass fraction profiles with experimental ones. This comparison is then extended to spray angles and vapor penetrations. The influence of injection boundary conditions such as injection rate profile and injection delay, on transient LES results is then evaluated. Finally, guidelines for simulating transient Diesel sprays in engines with LES are proposed.*

INTRODUCTION

In the past few years, Large Eddy Simulation (LES) has known a growing interest from the automotive community because of its unique capability to reproduce unsteady and sporadic phenomena like Cycle-to-Cycle Variations (CCV) [1-4] or abnormal combustions [5] in Spark Ignition (SI) engines. In the Diesel context, LES may be used to better predict pollutant emissions such as soots, which are highly dependent on the local air-fuel mixing process, and their CCV or to study transient operations like cold starts. However, up to now, such engineering issues were not properly addressed by LES, notably because detailed spray models and validations were needed.

A specificity of Diesel injection is that thermodynamic conditions are severe (injection pressure up to 2 500 bar) and that the introduction rate is often split into several sub-injections, leading to highly unsteady behaviours. However, most of preceding works on LES of Diesel sprays [6-11] were oriented towards quasi-steady behaviours in very long injection cases, also neglecting injection to injection variability effects. Therefore, dedicated studies have to be performed to assess the ability of LES models to correctly predict spray evolutions and cyclic variations in more realistic Diesel conditions.

The objective of this work is to perform detailed LES validations of transient Diesel sprays using the Eulerian-Eulerian approach developed by Simonin [12] and by Fevrier *et al*. [13] and further adapted to engine conditions by Martinez *et al*. [6, 14, 15]. For this purpose, dedicated experiments conducted at IFP Energies nouvelles in a high pressure vessel are used. Single and double injections are simulated, and comparisons are made with experimental fuel concentration profiles as well as penetration lengths and angles for a number of injection events. The impact of mesh refinement or boundary conditions at the injection patch is also discussed, and recommendations for future LES studies in Diesel engines are finally drawn.

1 EXPERIMENTAL SETUP

The experimental configuration is a direct Diesel injection in a high-pressure, high-temperature cell from IFP Energies nouvelles [16]. The injector, with a nozzle diameter of 0.2 mm, is situated in the center of the upper face of the cell (*Fig. 1*). This 1.4 L vessel is considered as wide enough to ensure a constant pressure. The mixture injected is composed of 70% of *n*-decane and 30% of α-methylnaphthalene.

Several configurations of this vessel have been experimentally studied, with or without the insertion of a
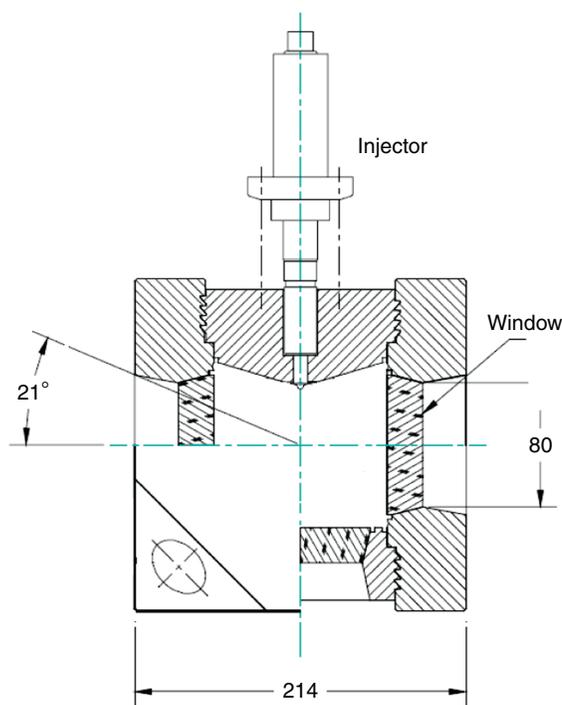

Figure 1

Experimental high pressure vessel (from Bruneaux and Maligne [16]).

fused silica plate in the center of the cell to reproduce spray-wall interactions. This article however focuses on the analysis of free jets evolving into quiescent nitrogen medium (no combustion). This experimental setup is particularly adapted to the assessment of LES spray models, because dedicated optical diagnostics have been performed over a large number of injections to retrieve average quantities and fluctuations as well. Notably, visualizations of the vapor phase have been obtained using Laser Induced Exciplex Fluorescence (LIEF). This technique here gives access to axial and radial fuel concentration profiles, which are key inputs for the simulation of Diesel spray combustion.

Experimental conditions representative of real Diesel engine operation have been selected in this paper, and two injection strategies have been investigated (*Tab. 1*).

Figures 2 and 3 present experimental injection rate evolutions in function of time for the two strategies. These profiles are obtained using an *EMI* apparatus measuring the liquid momentum at the nozzle exit. Such measurements exhibit very high levels of fluctuations, which are not physical – negative values are even found at the nozzle closure – and are therefore filtered to obtain the presented profiles.

TABLE 1

Experimental conditions

Injection pressure	1 200 bar
Vessel pressure	66.75 bar
Liquid temperature	400 K
Vessel temperature	950 K
Liquid density	791 kg/m^3
Gas density	25 kg/m^3
Single injection duration	0.3 ms
Double injection durations	0.3 ms / 0.28 ms
Double injection dwell time	0.4 ms

However, it is today recognized that such a filtering operation can alter the real signal in transient phases. Due to these uncertainties, it is generally chosen to use simplified profiles in CFD calculations with, for instance, trapezoidal shapes. In this work, the same methodology has been followed by using a constant flow rate in the fully-opened phase and a constant slope during needle closure. However, the experimental opening profile has been used in order to get a more physical behaviour during this highly transient phase (*Fig. 2, 3*) and the injection timing has been adjusted to guaranty that the right fuel mass has been introduced in the vessel. The implications of all these choices on LES results should nevertheless be taken into consideration and will be discussed in Section 4.
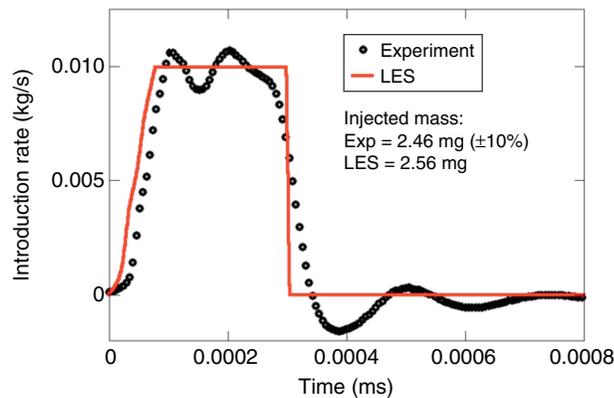

Figure 2

Injection mass flow rate for the single injection case.
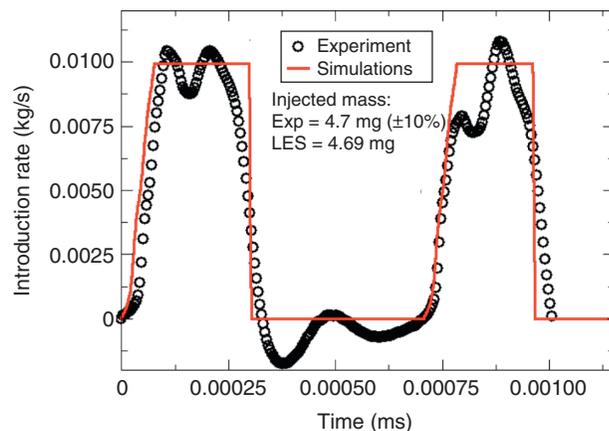
Figure 3

Injection mass flow rate for the double injection case.

2 LES SPRAY MODEL

2.1 The Eulerian – Eulerian Approach

Both gas (air and evaporated fuel) and liquid (injected fuel) phases are modeled using an Eulerian formulation and are two-way coupled through the drag force. As the vessel temperature is 950 K, the spray is vaporising and mass and heat transfer model are used. The gas phase is solved by compressible Navier-Stokes equations, and the Eulerian conservation equations for the liquid are based on the Mesoscopic Eulerian Formalism developed by Fevrier *et al.* [13].

An important feature of this formalism is that it introduces the concept of Random Uncorrelated Motion. The velocity of droplets is decomposed in two parts: a statistical Eulerian velocity shared by all droplets (the correlated velocity) and a residual velocity component (the uncorrelated velocity) specific to each droplet. The correlated mean motion is tracked by a set of equations for momentum, whereas the Random Uncorrelated Motion is tracked by its energy in a new conservation equation interacting with the correlated motion by shear and compression effects. The formalism proposed by Fevrier *et al.* [13] was designed for diluted sprays. Martinez *et al.* [6] proposed an extension of this model to dense sprays by taking into account collisions between droplets.

2.2 The DITurBC Model

Previous equations have been adapted to dense flows, but the Eulerian/Eulerian approach can today hardly be applied to the nozzle region. Complex interactions between multiple phenomena, like primary atomization, cavitation or turbulence, occur at the injector tip, and

resolving all this physics would indeed necessitate additional models and very refined meshes. LES calculations would require huge CPU costs, inaccessible to industrial use.

A convenient way to overcome this issue was previously proposed by Martinez *et al.* [14], and consists in moving the inlet boundary condition downstream from the real injector nozzle. This approach, called model DITurBC (Downstream Inflow Turbulent Boundary Condition), allows to avoid computing the dense region of the spray.

DITurBC is based on the assumption that physics in the region close to the injector can be reproduced at a certain distance D of the real nozzle, and without impacting deeply the physics downstream. This distance depends on injector parameters, but often corresponds to ten injector hole diameters. This modification is made possible by the addition of a cone at the nozzle exit, and the inlet boundary condition becomes the DITurBC plane (*Fig. 4*).

On this plane, the liquid and gas velocities, enthalpy, Random Uncorrelated Energy (RUE), number and diameter of droplets are imposed as Gaussian profiles.

The droplet size profile mentioned previously, allows to partially taking into account the atomization process. Actually, this phenomenon is mainly localized in the unsimulated DITurBC cone, and therefore no atomization model is used in the LES computations.

Figure 4

Visualization of DITurBC plane.

Another modeling aspect is the spray/flow interactions. In the nozzle region, these interactions are not solved and therefore need to be modeled to account for turbulence generation in this area. To achieve this aim, turbulent profiles for gas and liquid velocity are imposed on the DITurBC plane.

In order to generate such a turbulent field with a given statistical profile, a non-dimensional homogeneous fluctuating velocity field is generated. This field is then rescaled, added to the mean Gaussian velocity profile, and imposed on DITurBC for both liquid and gas phases. This turbulence generation method is based on the work of Kraichnan [17] and a similar method is used by Smirnov *et al.* [18]. The divergence free, statistically stationary, homogeneous, isotropic, multivariate-normal velocity field, for N modes, is of the form:

$$v_i(x,t) = \sqrt{\frac{2}{N}} \sum_{n=1}^{N} \left[\begin{array}{c} p_i^{(n)} \cos\left(k_e \lambda^{(n)} x_j + \omega^{(n)}\right) \\ + q_i^{(n)} \sin\left(k_e \lambda^{(n)} x_j + \omega^{(n)}\right) \end{array} \right] \quad (1)$$

where $p_i^{(n)} = \varepsilon_{ijm}\xi_j^{(n)}\lambda_m^{(n)}$ and $q_i^{(n)} = \varepsilon_{ijm}\varsigma_j^{(n)}\lambda_m^{(n)}$. Here, ε_{ijm} is the permutation tensor used in the vector-product operation. The variables $\xi_j^{(n)}$, $\varsigma_j^{(n)}$ and $\lambda_m^{(n)}$ are random quantities $\xi_j^{(n)}$ and $\varsigma_j^{(n)}$ are calculated from normal distribution $N(0,1)$, *i.e.* with a mean of 0 and a standard deviation of 1. $\lambda_m^{(n)}$ is calculated from a Gaussian distribution $G(0,1/2)$. For an infinite number of modes, the energy spectrum is of the form:

$$E(k) = \frac{2}{3} 16\sqrt{\frac{2}{\pi}}\left(\frac{k}{k_e}\right)\exp\left(-2k^2/k_e^2\right) \quad (2)$$

with a maximum energy for $k = k_e$ and a correlation length of the order of $L_e = 1/k_e$. In the paper of Kraichnan [17], $\omega^{(n)}$ is obtained from a Gaussian distribution with a standard deviation ω_0 leading to a time correlation of the form $\exp\left(-\omega_0^2 t^2/2\right)$. Here, a different approach is used. Instead of generating a 2D inlet field varying with time, a 3D field, *i.e.* 2D inlet + direction perpendicular to the inlet, is generated. At each time t, the field corresponding to the 2D section located at a distance $U_{conv}.t$ upstream the inlet section (in the direction perpendicular to the inlet) is injected, where U_{conv} is the mean velocity in direction perpendicular to the inlet plane. One can view the turbulent velocity field as velocity fluctuations in a grid turbulence with mean velocity U_{conv}.

From the homogeneous isotropic turbulent velocity field, an inhomogeneous fluctuating target velocity U_i^T is created to reproduce the statistical mean velocity U_j,
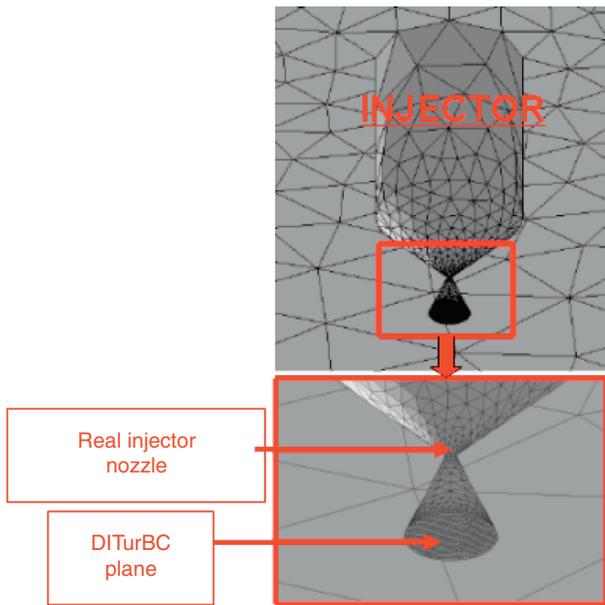
the Root-Mean-Square (RMS) fluctuations $\sqrt{\langle u_i'^2 \rangle}$ and the cross correlations $\langle u_i' u_j' \rangle$, using the tensor a_{ij} [19]:

$$U_i^T(x,t) = \langle U_i(x) \rangle + a_{ij}(x) v_j(x,t) \qquad (3)$$

This allows obtaining an anisotropic field, more relevant for a jet simulation. The RMS fluctuations u_{rms}, v_{rms} and w_{rms} are set to fit the turbulence intensity of a gas jet in the self-similarity area according to [20, 21], i.e. $u_{rms}/\langle U \rangle_{axis} = v_{rms}/\langle U \rangle_{axis} = w_{rms}/\langle U \rangle_{axis} = 0.2$. A questionable point here is how to set the level of correlation between the gas and the liquid fluctuations. For the sake of simplicity and in a first approach, no correlation is supposed and the amplitude of the velocity fluctuations is assumed equal for the gas and the liquid phase.

3 LES OF SINGLE AND DOUBLE INJECTION EVENTS

3.1 Numerical Setup

Simulations have been performed with the AVBP LES code developed by IFP Energies nouvelles and CERFACS, which solves Navier-Stokes compressible equations for reactive two-phase flows [22]. All cases have been run with the second order Lax-Wendroff explicit scheme, centered in space and time, and with the constant Smagorinsky model for Sub-Grid-Scale (SGS) turbulence. In addition, three unstructured meshes have been built with different refinement levels to validate the convergence of LES results (*Tab. 2*). The refinement effort has been focused on the spray region (up to 54 mm under the nozzle, see *Fig. 5*), while a very coarse mesh has been used elsewhere to reduce CPU time without impacting the spray development.

3.2 LES Quality Analysis and Assessment on the Single Injection Case

3.2.1 Injection to Injection Variability

At the nozzle exit, the spray is highly turbulent, and the randomness of the turbulence is assumed to be responsible for differences between each experimental injection. Because running two LES with the same parameters gives the same results, a random drawing should be modified from one simulation to another. This operation is performed by modifying the initial seed value in the random number generator of DITurBC.

Figure 6 presents four instantaneous vapor fields at 500 s after the Start of the Injection (SOI): two are taken

TABLE 2

Meshes parameters (cell characteristic size and number)

	Mesh 1	Mesh 2	Mesh 3
Injector tip zone	80 μm	80 μm	80 μm
Bottom of the refined zone	1 200 μm	600 μm	300 μm
Number of cells	0.5M	1.8M	6.75M

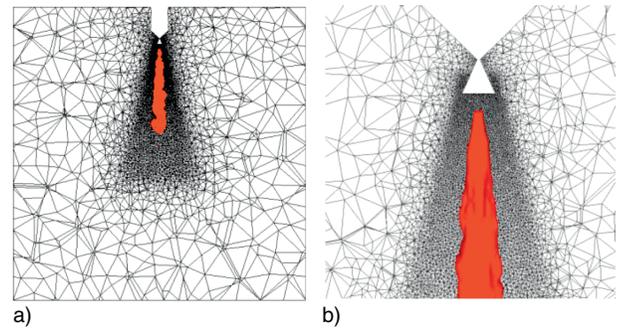a)   b)

Figure 5

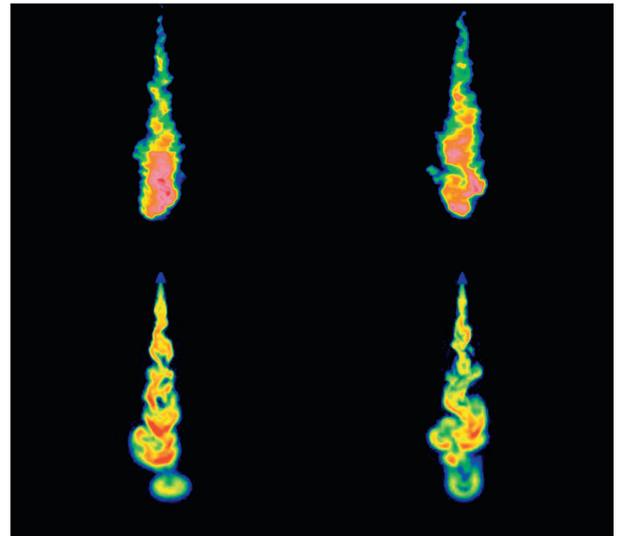LES reference grid (Mesh 2). a) General view of the vessel, b) near nozzle zone.

Figure 6

Instantaneous fuel concentration fields (kg/m^3) at 500 μs after SOI for two different realizations: experiment (top) and LES (bottom - Mesh 2).

from experiments (top) and two from LES (bottom) obtained using Mesh 2. First of all, the simulated spray structures look quite close to experimental ones, notably the spray angle, penetration and large scale distortions are correctly represented. In addition, comparing the two LES realizations, this structure is clearly affected by turbulence injection, which confirms the potential of the turbulence injection method to mimic injection to injection variability. Nevertheless, the qualitative agreement between simulations and experiments is not perfect. Notably experimental vapor fields seem smoother than numerical ones, especially because of the presence of smaller structures inside the spray, and also due to the filtering operation needed to reduce noise from the raw experimental images. Moreover, a pocket of vapor is present at the leading edge of the spray in the LES, while being not observed experimentally. These differences will be discussed further in this paper.

It should also be noticed that the observed variability seems high, indicating that a quite large number of realizations should be simulated to get a reasonable statistical convergence. This is confirmed by Figure 7, which presents axial fuel concentration profiles along the spray axis. At a given instant, the local variability between two injection events can indeed be higher than 100% compared to the mean, due to intermittency effects in the spray. Figure 8 presents mean axial fuel concentration profiles with their corresponding variances. The good agreement between numerical and experimental variance highlights that the LES turbulent field reproduces quite well the variability induced by the natural randomness of turbulence.

In order to evaluate statistical convergence requirements, a sensitivity analysis of LES results has been performed by comparing mean fuel concentration fields for a different number of realizations at 500 µs after SOI (*Fig. 9*). It is evidenced that the convergence is already correct for 15 injections and clearly reached for 30 injections. This observation is confirmed by Figure 10, where mean axial fuel concentration profiles are plotted using respectively 15, 30 and 50 realizations. Consequently, it was decided to keep the value of 30 injections in the following of this section.

3.2.2 Mesh Convergence

Convergence of LES results is a critical criterion to assess the reliability of simulations and does not only concern statistics but also mesh resolution. This point is very important for the validation of spray models, but also to provide guidelines for future practical application of LES in Diesel engines. To this end, LES have been conducted for three grid resolutions (*Tab. 2*), and analyses
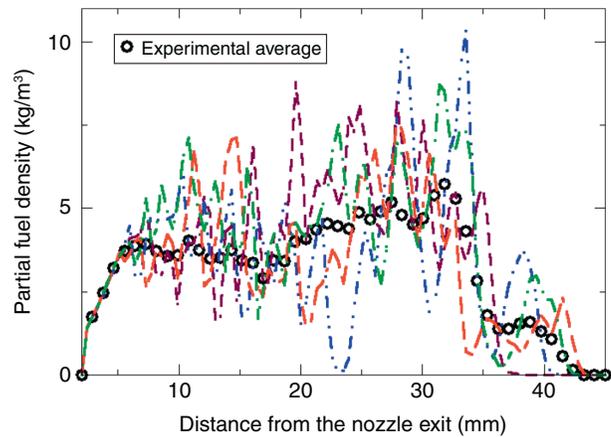

Figure 7

Axial partial fuel density at 500 µs after SOI: experimental average profile (circle) and four instantaneous profiles for different LES injections (lines – Mesh 2).
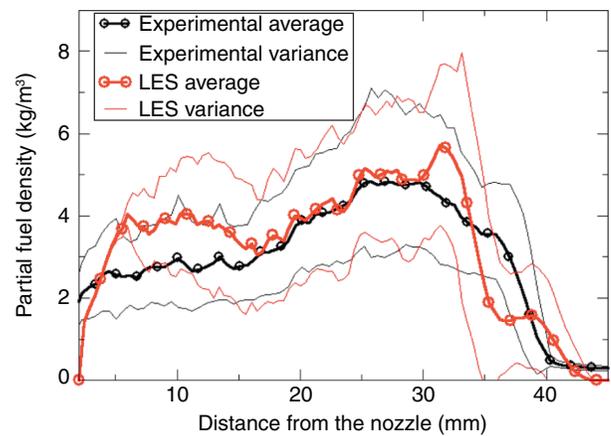

Figure 8

Axial partial fuel density at 500 µs after SOI: experimental and LES average profiles with their respective variances.
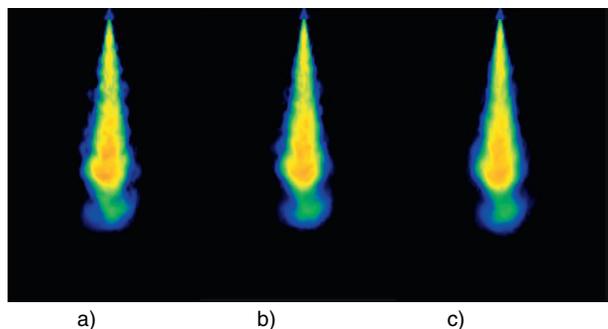

Figure 9

Mean fuel concentration fields on Mesh 2 for a different number of realizations at 500 µs after SOI. a) 15, b) 30, c) 50 realizations.
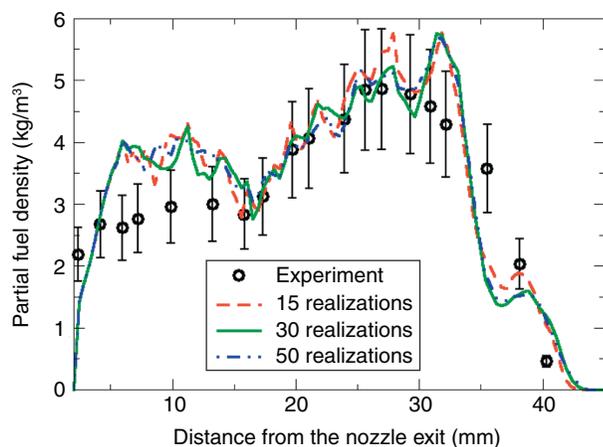
Figure 10

Mean axial fuel concentration profiles at 500 μs after SOI, for the three different numbers of LES realizations.

Figure 11

Numerical mean fuel concentration fields for the three different meshes, compared to the experimental one (500 μs after SOI). a) Experiment, b) Mesh 1 (0.5M cells), c) Mesh 2 (1.8M cells), d) Mesh 3 (6.75M cells).

Figure 12

Instantaneous fuel concentration fields for the three meshes at 500 μs after SOI. a) Mesh 1, b) Mesh 2, c) Mesh 3.

are carried out on the base of thirty realizations for statistical convergence, as discussed in the previous section. It should however be noticed that fifty images were needed to build experimental vapor fields and profiles.

Figure 11 presents experimental and simulated mean fuel concentration fields for the three meshes. It is first evidenced that statistical convergence is not fully reached for the finer grid. 50 realizations would probably be necessary to provide converged averages, but this has not been carried out because of the high CPU cost required. This number is consistent with experimental results which needed 50 images to get a correct mean vapor field. On the contrary, the reference and coarse meshes lead to a fast convergence, probably because of a lack of small turbulence structures in the spray, which are highly dissipated when propagating downstream. This statement can be verified in Figure 12, which presents instantaneous vapor fields for the three meshes. The spray shape indeed shows small distortions for Mesh 3, which could be compared to those found in experiments, while larger structures are found for Mesh 2 and even more for Mesh 1.

Quantitative comparisons between the different meshes are presented in Figures 13 and 14, where axial and radial fuel partial density profiles are plotted.

It is first evidenced that grid convergence is not obtained for Mesh 1, which exhibits a different behaviour from the two finer grids. Indeed, fuel concentration is higher in the near nozzle area, while a pick of concentration is found at the leading edge of the spray both for Mesh 2 and 3 and in experiments. This behaviour may be due to a lack of spray perturbations captured with Mesh 1, leading to a more stable jet, a higher penetration
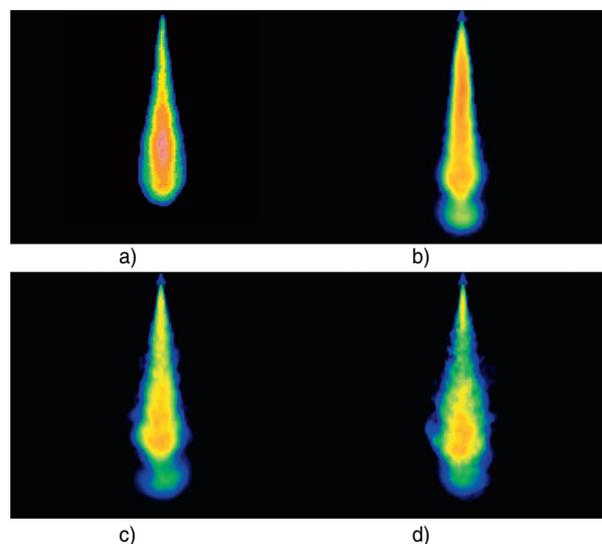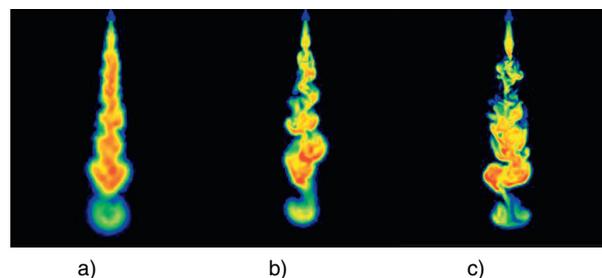
and a low vaporization at the leading edge of the spray. On the contrary, Mesh 2 and 3 provide quite close results, even if results from Mesh 3 are statistically not fully converged.

These results are in addition very close to experimental data, namely the peak of axial fuel concentration is correctly reproduced (*Fig. 13*) and the radial profile is well described (*Fig. 14*). However, an overestimation of the fuel concentration can be noticed in the few millimetres downstream the injector nozzle. This behaviour will be analysed in details in Section 4.

Other classical simulation validation criteria concern spray angle and penetration. Using these criteria is however more tricky, because results depend a lot on
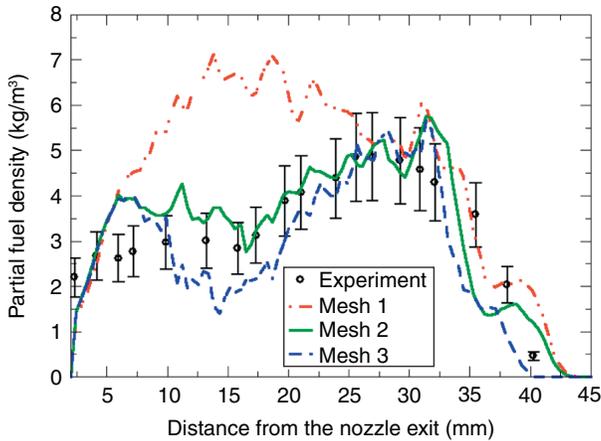
Figure 13

Mean fuel axial profiles at $t = 0.5$ ms after SOI, for the three LES meshes.
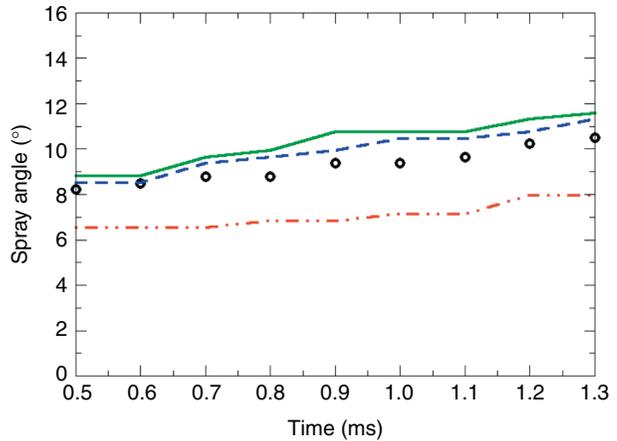

Figure 15

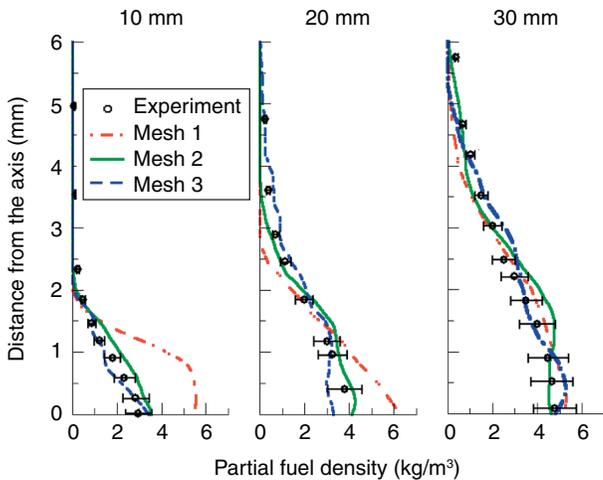Spray angle evolution for the three LES grids and comparison with experiments.

Figure 14

Mean fuel radial profiles at different position downstream the nozzle at $t = 0.5$ ms after SOI, for the three LES meshes.
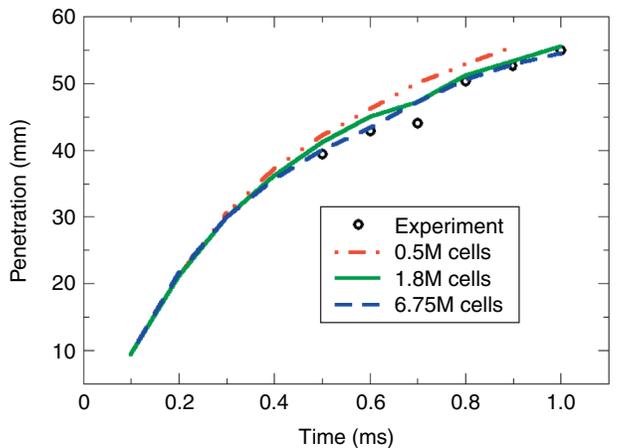

Figure 16

Spray penetration evolution for the three LES grids and comparison with experiments.

threshold values used to define them. Experimental uncertainties have therefore to be considered, especially in the near nozzle region where liquid fuel can be found. In the present case, a threshold of 0.5 kg/m^3 has been chosen both for experiments and simulations, and comparisons on the angle are only performed after the end of the evaporation process, namely from 500 µs after SOI.

Figures 15 and 16 present transient spray angle and penetration evolutions for the three LES grids. Previous observations are confirmed, *i.e.* LES results are not converged for Mesh 1, especially regarding the spray

angle, which is smaller than for the two other grids due to a too stable jet. This behaviour also implies a too high penetration, notably after the end of injection. Once again, Mesh 2 and 3 give comparable values both for the angle and penetration, which are also very close to experimental measurements.

Finally, it can be considered that LES results are well converged using Mesh 2 and thirty realizations. That is why this set-up will be retained in the following, with the idea to optimize both CPU costs and convergence quality.

3.2.3 LES Quality Assessment

An important question regarding LES is to know if a sufficient part of the turbulent flow energy is directly resolved by the computational grid. In this case, it is considered that the biggest scales of the flow, which behaviour is difficult to model using a SGS model, are well captured, then conferring a high level of confidence in the LES predictivity. A convenient criterion to analyse LES quality is based on the work of Pope [23]. Following this approach, the ratio of the SGS flow energy over the total turbulent energy is evaluated as:

$$\frac{K_{sgs}}{K_{total}} = \frac{K_{sgs}}{K_{sgs} + K_{turb}} \quad (4)$$

where the turbulent kinetic energy K_{turb} is given by:

$$K_{turb} = \frac{1}{2} \left(u_{rms}^2 + v_{rms}^2 + w_{rms}^2 \right) \quad (5)$$

and u_{rms}, v_{rms} and w_{rms} are the components of the root mean square velocity. The SGS kinetic energy is obtained from the SGS turbulent viscosity v_t following:

$$K_{sgs} = \left(\frac{v_t}{C_k \Delta} \right)^2 \quad (6)$$

with $C_k = 0.1$ and Δ the local characteristic length scale of the grid given by the cube root of the cell volume. Finally, the Pope criterion is satisfied when the SGS kinetic energy is less than 20% of the total turbulent energy.

Figure 17 presents a field of the ratio defined by Equation (4) on a vertical plane through the injector axis for Mesh 2. A threshold has been set at the value 0.2 to visualize more clearly the zone where the Pope criterion is satisfied. The computational grid located on the left of the figure allows to conclude that the mesh resolution is sufficient because the energy ratio is lower than 0.2 within the spray. Out of this area, the mesh is coarsened, and the ratio is close to 1 due to the presence of very large cells. The results are not affected by this choice, because there is no physics to solve in these regions.

This single injection case highlights the potential of predictability of LES to represent Diesel direct injection in engine conditions. It also allows to define first design rules for LES meshes and guidelines regarding statistical convergence. Indeed, a minimum resolution corresponding to Mesh 2 (see *Tab. 2*) is needed to correctly solve the largest scales of the spray during its propagation. In this case, at least fifteen realizations have to be computed to establish mean vapor fields, thirty realization being however an optimal value. Finally, refining the grid implies
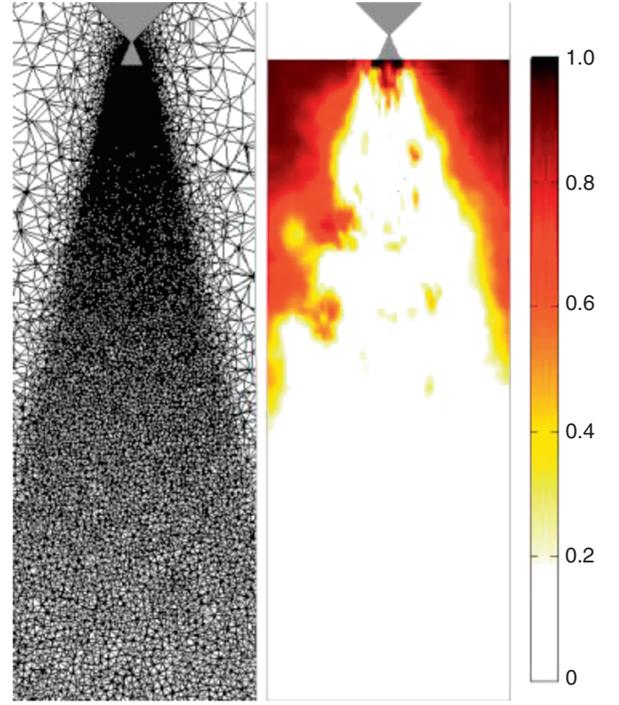

Figure 17

LES quality analysis: kinetic energy ratio $\left(K_{sgs}/(K_{sgs} + K_{turb}) \right)$ at the end of injection.

the computation of a high number of injection events to get converged mean vapor fields.

3.3 Application to a Double Injection Configuration

The double injection test case, which seems similar to the single injection one, is actually quite different due to the physics generated by the consecutive injections. The second spray is indeed injected in the wake of the first one, and the entrainment generated by the first injection modifies all the spray structure compared to a single injection in a quiescent vessel. The first idea followed in this section is therefore to evaluate if guidelines established for the single injection configuration are still valid when dealing with split injection cases. All the following simulations are thus performed using Mesh 2, and averages are based on fifteen realizations.

Figure 18 compares experimental and numerical mean axial vapor fields, 1.25 ms after SOI. Despite a more complex physics, numerical results are coherent with the experiments, both in terms of fuel concentration levels and spatial evolution. Notably, the two concentration peaks corresponding to the leading edges of the two sprays are well predicted. These results are confirmed
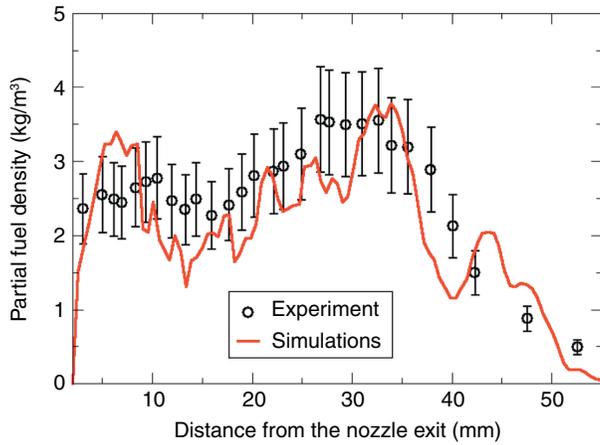
Figure 18

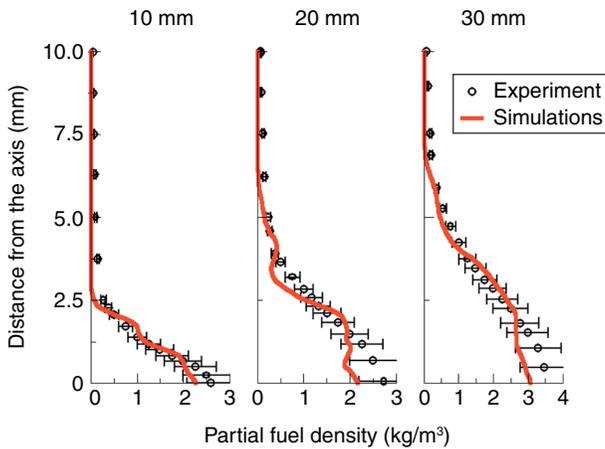Mean fuel axial profiles at $t = 1.25$ ms after SOI, for the double injection configuration.

Figure 19

Mean fuel radial profiles at $t = 1.25$ ms after SOI, for the double injection configuration.

Figure 20

Mean fuel concentration fields at $t = 1.25$ ms after SOI, for the double injection configuration.

by Figure 19, which presents radial profiles at different location downstream the injector nozzle. The agreement between LES and experiments is very satisfactory, and differences stay within experimental uncertainties.

Nevertheless, the fuel concentration overestimation in the injector nozzle zone, already observed for the single injection, is still observed in Figure 18 and will be discussed in Section 4.

Despite the correct agreement between experimental data and LES, it should be noticed that the number of realizations defined for the single injection case seems to be underestimated for this double injection configuration, as the mean fuel concentration fields are not fully converged (*Fig. 20*). The convergence was not
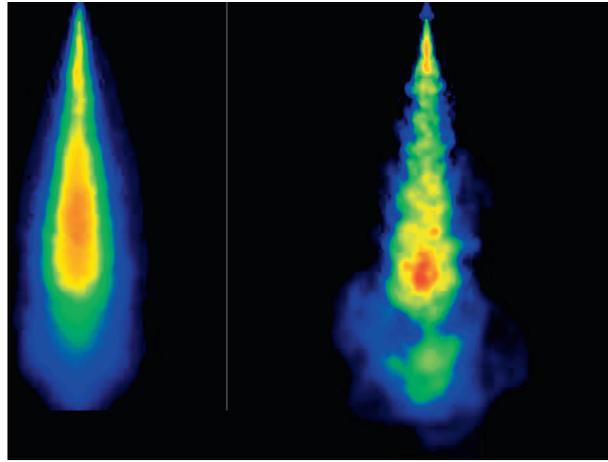
investigated further in thus study, but it is believed that a minimum of thirty injection events should be computed to reach convergence. This statement should thus be taken into account for future studies of Diesel injection and combustion in engines.

4 TRANSIENT PHASES IMPACT ANALYSIS AND MODELING ISSUES

Even if a quite good agreement has been found between experiments and simulations in the previous section, some potential errors have been observed both on the single and double injection configurations. The origins of these errors are difficult to identify from the previous results, notably because high experimental uncertainties exist regarding boundary conditions and could affect LES. In particular, strong approximations are generally made on the real injection rate profile, which is a direct input for the simulation. The raw signal extracted from the injector test bench is indeed highly perturbed by oscillations from the sensor itself (*Fig. 21*). Such noise is classically removed by filtering the signal, but this operation can also alter the injection rate profile, especially in highly transient phases like the injector opening and closure, where steep evolutions exist. The influence of filtering operation during the fully opened phase is not analyzed in this study, and a constant introduction rate profile is used for LES computations. However, it is important to keep in mind that it could be a way of uncertainty. Another consequence of this filtering operation is that the injection timing can be slightly modified,
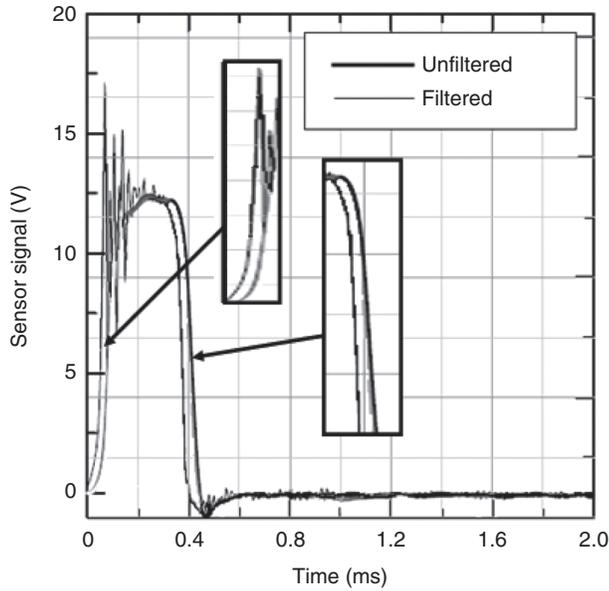
Figure 21

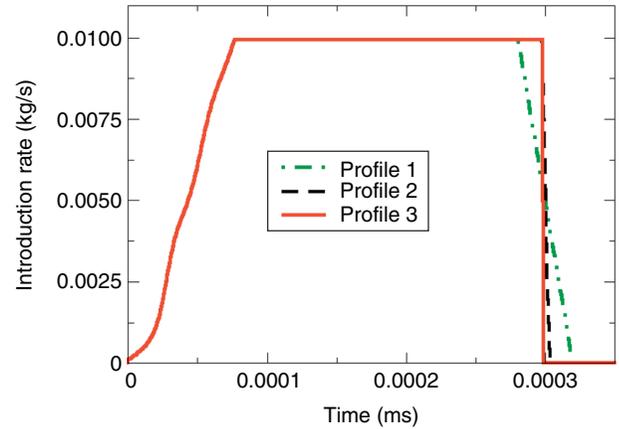Raw and filtered signal for the single injection case.

Figure 22

Injection rate profiles for three injector closure slopes.

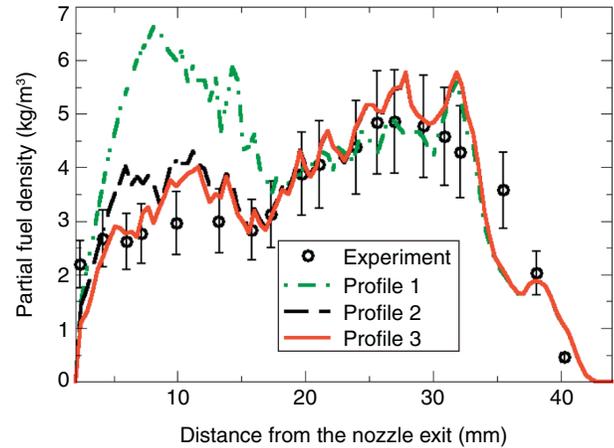
Figure 23

Mean fuel axial profiles at $t = 0.5$ ms after SOI, for a single injection (mean achieved on 15 realizations).

so that offsets in time might be considered to compare experiments and simulation. It should also be noticed that the idea of moving the injection plane inside the simulation domain, while boundary conditions are in reality only known on the injector nozzle, can lead to additional offsets. For all these reasons, it was decided to perform a specific study with the aim to evaluate the effect of these uncertainties on numerical results, and to better identify possible modeling issues of the approach followed in this work.

4.1 Sensitivity to the Injection Rate Profile

Transient phases of injection present great uncertainties about the real injection rate profile, especially during closure, characterized by a very fast decrease of the injection rate. Filtering this signal often leads to unphysical negative values but also to a quite low slope compared to the raw signal. In practice, the injection rate in therefore generally clipped and the closure slope is modified to be more coherent with the experimental signal (*Fig. 2*). The choice of this slope is however questionable, notably because it may have an important impact on mixing processes in the wake of the spray; indeed, a low slope will induce low liquid velocities and low mixing, fostering high fuel concentration zones near the injector nozzle after injection.

In order to analyze the effect of the closure slope on the spray evolution, LES have been performed with three different values (*Fig. 22*): slope 1 corresponds to the reference value previously used (closure in 38 μs), slope 2 is slightly steeper (6.2 μs) and the last slope is an unphysical instantaneous closure, considered as a limiting case. The closure time is changed in consequence in order to keep the same injected fuel mass. Figure 23 presents evolutions of the mean fuel axial profiles based on fifteen realizations and Mesh 2 for each case. It is first observed that the closure slope has an important impact on the fuel concentration field, not only in the injector nozzle area, but also quite far from this region because

of entrainment effects from the leading edge of the spray. In addition, steep slopes, more coherent with the raw experimental signal, allow to correctly match experimental results in the near nozzle area. However, the fact that slope 3 brings some improvements on the fuel concentration profile compared to the reference slope 1 should not be considered as a physical behaviour because the injector closure is instantaneous. This point will be discussed further in Section 4.3.

The same kind of study has been performed regarding the opening slope with the aim to improve fuel concentration profiles at the leading edge of the spray (not shown). However, whatever the slope, the fuel pocket observed in this region still exists. It was also observed that this pocket is less pronounced when increasing the mesh resolution and mainly appears when the spray reaches low resolution zones. It is then believed that this behaviour may not be linked to errors on the injection rate profile, but to excessive diffusion at the leading edge of the spray leading to fuel accumulation in this zone.

4.2 Impact of the Visualisation Timing

Uncertainties regarding injection boundary conditions do not only concern profiles but also the real injection timing. A first source of error is the response time of the injector. For instance, for the single injection case, the duration of the injector order is 500 μs whereas the real injection time is about 300 μs. Other approximations can be done on introduction rate measurements because the sensor used also has a response time. The same observation can be done for the uncertainty of camera response and exposure time which provides the images used to obtain experimental fuel concentration profiles. Finally, filtering the raw signal also alters this timing (*Fig. 21*). However, comparing experimental and numerical fields which do not have exactly the same timing can lead to huge fictive errors. This is particularly important for comparisons performed at the injector closure because of the very fast decrease of velocity [24]. In this case, an error of several ten microseconds could have a great impact on the fuel concentration field.

In order to evaluate the impact of timing uncertainties on LES analysis, mean fuel concentration profiles have been plotted at different instants around 500 μs after SOI (*Fig. 24*). It is highlighted that an error of 30 μs has a non-negligible influence on the fuel field evolution. Notably using a timing of 530 μs after SOI gives a better agreement between simulations and experiments in the wake of the spray. Nevertheless, the matching is still not perfect indicating that some improvements should be brought to the spray model.
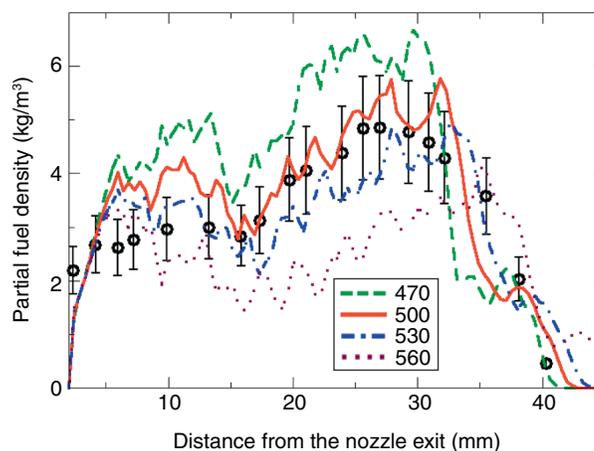

Figure 24

Mean fuel axial profiles at different instants: 470 (- - -), 500 (–), 530 (– · –) and 560 (…) μs after SOI, for a single injection (mean achieved on 15 realizations).

4.3 DITurBC Modeling Issues

Considering previous discussions, all differences between LES and experiments could not be attributed to uncertainties on boundary conditions. Indeed, whatever the assumption about the signal to impose on the DITurBC plane some errors remain, especially in zones where transient effects are important, *i.e.* at the leading edge and in the wake of the spray.

It is known that air entrainment in the near nozzle zone plays an important role in the mixing process. However, this phenomenon is highly affected by the use of DITurBC because it is not directly resolved on the mesh. Part of these effects is modeled by the use of turbulence injection both on liquid and gas (*Sect. 2.2*), but the idea of moving the boundary condition downstream the nozzle naturally imposes geometrical constraints to the flow. This modification leads to recirculation zones at the edges of the DITurBC plane (*Fig. 25*), especially at the end of injection, when the flow velocity is low. Stagnation zones are then generated, and fuel is unphysically accumulated in the wake of the spray. Steepening the injector closure slopes in an exaggerated manner (see slope 3, *Sect. 4.1*) is a way to recreate the lack of entrainment by maintaining high flow velocities up to the end of injection, that's why results were improved in this case.

Another important approximation concerns the validity of the turbulence injection model during transients. Indeed, the RMS perturbation levels (20%) have been extracted from fully developed sprays, while higher levels
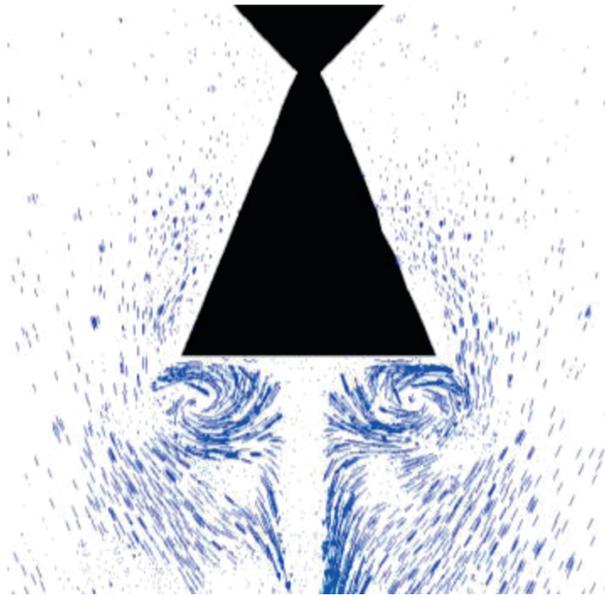
Figure 25

Velocity vectors close to the injector patch at 0.5 ms after SOI.

could be expected during closure and opening. This may allow to enhance air entrainment and mixing in these phases and to reduce accumulation effects observed in the LES, avoiding to modify injection profiles.

CONCLUSION

This paper was dedicated to LES simulations of transient Diesel sprays using an Eulerian/Eulerian formalism to describe two-phase flows, and the DITurBC model to account for Diesel injection physics in the near nozzle area. Two configurations were computed, namely single and double injection cases, to be representative of real Diesel-engine strategies. Injections were performed in a quiescent vessel, and LIEF measurements allowed to compare LES with fuel concentration fields and profiles in different locations as well as spray angles and penetration.

In a first part, tests were performed on the single injection case to define an optimal numerical setup. Notably mesh and statistical convergence were studied, showing that the mesh should not be coarsened too rapidly downstream the injector nozzle, and that the number of LES realizations to compute to get converged averaged profiles depends on the mesh resolution. These tests allowed retaining an intermediate mesh resolution (Mesh 2), and a minimum number of realizations of fifteen to establish reliable statistics, spray penetration and angle. This setup finally allowed a good agreement between experiments and simulations, the main discrepancies being found in the highly transient phases. It was then used to compute the two-injection case and allowed to obtain a quite good agreement with experimental fuel concentration fields, while the physics of the second injection is quite different from the first case. Nevertheless results were not fully converged and indicate that the realization number should be increased in multiple injection cases.

The second part of the paper was devoted to a more detailed analysis of the effect of experimental uncertainties on LES results, with a special focus on transient phases, where simulation errors are found. The influence of the injection rate profile was evaluated modifying the injector closure slope and demonstrated that numerical results can be highly affected by the flow velocity evolution at the boundary condition. It was also shown that uncertainties on the real injection timing can affect comparisons between LES and experiments because of the very fast evolution of the fuel concentration field after injection closure. Consequently the quality of injection rate measurements can have a very great impact on simulation results and analysis of transient phases. A special care has to be devoted to such cases. Finally, some modeling issues of the DITurBC injection model were highlighted. The idea to move the injection plane inside the computational domain indeed generates recirculation zones during injector closure, explaining part of the fuel accumulation phenomenon observed in the LES. An idea to limit this effect could be to steepen in an unphysical manner the injector slope closure to avoid low velocities at the end of injection. A more physical way to solve such problems both at the leading edge and in the wake of the spray, could be to modify turbulence injection properties in transient phases. The velocity fluctuation levels imposed were indeed extracted from fully developed sprays and may be underestimated during injector opening and closure.

Despite some modeling limitations, the presented results are however very encouraging for application of such two-phase flow models for LES of Diesel engines. This approach will be used at IFP Energies nouvelles in a near future to perform LES of combustion in the same vessel and in a Diesel engine configuration.

REFERENCES

1 Richard S., Colin O., Vermorel O., Benkenida A., Angelberger C., Veynante D. (2007) Towards large eddy simulation of combustion in spark ignition engines, *Proc. Combust. Inst.* **31**, 2, 3059-3066.

2 Vermorel O., Richard S., Colin O., Angelberger C., Benkenida A., Veynante D. (2009) Towards the understanding of cyclic variability in a spark ignited engine using multi-cycle LES, *Combust. Flame* **156**, 1525-1541.

3 Enaux B., Granet V., Vermorel O., Lacour C., Thobois L., Dugue V., Poinsot T. (2011) Large Eddy Simulation of a motored single-cylinder piston engine: numerical strategies and validation, *Flow Turbul. Combust.* **86**, 2, 153-177.

4 Granet V., Vermorel O., Lacour C., Enaux B., Dugué V., Poinsot T. (2012) Large-Eddy Simulation and experimental study of cycle-to-cycle variations of stable and unstable operating points in a spark ignition engine, *Combust. Flame* **159**, 1562-1575.

5 Lecocq G., Richard S., Michel J.-B., Vervisch L. (2011) A new LES model coupling flame surface density and tabulated kinetics approaches to investigate knock and pre-ignition in piston engines, *Proc. Combust. Inst.* **33**, 6, 1215-1226.

6 Martinez L., Benkenida A., Cuenot B. (2007) Towards Large Eddy Simulation of Diesel Fuel Spray Using an Eulerian-Eulerian Approach, *ILASS-Europe*.

7 Vuorinen V., Hillamo H., Nuutinen M., Kaario O., Larmi M., Fuchs L. (2011) Effect of Droplet Size and Atomization on Spray Shape: A Priori Study Using Large-Eddy Simulation, *Flow Turb. Combust.* **86**, 533-561.

8 Vuorinen V., Hillamo H., Nuutinen M., Kaario O., Larmi M., Fuchs L. (2010) Large-Eddy Simulation of Droplet Stokes Number Effects on Turbulent Spray Shape, Atomization Sprays, **20**, 93-114.

9 Hori T., Senda J., Kuge T., Gen Fujimoto H. (2006) Large Eddy Simulation of Non-Evaporative and Evaporative Diesel Spray in Constant Volume Vessel by Use of KIVALES, *SAE Paper* 2006-01-3334.

10 Fujimoto H., Hori T., Senda J. (2009) Effect of Breakup Model on Diesel Spray Structure Simulated by Large Eddy Simulation, *SAE Paper* 2009-24-0024.

11 Vuorinen V., Larmi M. (2008) Large-Eddy Simulation on the Effect of Droplet Size Distribution on Mixing of Passive Scalar in a Spray, *SAE Paper* 2008-01-0933.

12 Simonin O. (1996) Combustion and turbulence in two phase flows. Lecture series 1996-02, Von Karman Institute of Fluid Dynamics.

13 Fevrier P., Simonin O., Squires K.D. (2005) Partitioning of particle velocities in gas-solid turbulent flows into a continuous field and a spatially uncorrelated random distribution: Theoretical formalism and numerical study, *J. Fluid Mech.* **533**, 1-46.

14 Martinez L., Vié A., Jay S., Benkenida A., Cuenot B. (2009) Large Eddy Simulation of Fuel sprays using the Eulerian Mesoscopic Approach. Validations in realistic engine conditions, *11th ICLASS International Conference on Liquid Atomization and Sprays Systems*, Vail, Colorado, USA.

15 Martinez L., Benkenida A., Cuenot B. (2010) A model for the injection boundary conditions in the context of 3D simulation of Diesel Spray: Methodology and validation, *Fuel* **89**, 1, 219-228.

16 Bruneaux G., Maligne D. (2009) Study of the Mixing and Combustion Processes of Consecutive Short Double Diesel injections, *SAE Paper* 2009-01-1352.

17 Kraichan R. (1970) Diffusion by a Random Velocity Field, *Phys. Fluids* **13**, 22-31.

18 Smirnov A., Shi S., Celik I. (2000) Random Flow Simulations with bubble dynamics model, *Proceedings of FEDSM00, ASME 2000 Fluids Engineering Division Summer Meeting*, Vol. FEDSM2000-11215, Boston, Massachusetts, USA.

19 Klein M., Sadiki A., Janicka J. (2003) A digital filter-based generation of inflow data for spatially developing numerical simulation or large eddy simulation, *J. Comput. Phys.* **186**, 652-665.

20 Hussein H., Capp S., Georges W. (1994) velocity measurements in a high-reynolds-number-momentum-conservative, axisymmetric turbulent jet, *J. Fluid Mech.* **258**, 31-75.

21 Chaves H., Kirmse C., Obermeier F. (2004) Velocity measurements of dense Diesel fuel sprays in dense airization, *Atomization Sprays* **14**, 589-609.

22 Moureau V., Lartigue G., Sommerer Y., Angelberger C., Colin O., Poinsot T. (2005) Numerical methods for unsteady compressible multi-component reacting flows on fixed and moving grids, *J. Comput. Phys.* **2020**, 2, 710-736.

23 Pope S.B. (2004) Ten questions concerning the large-eddy simulation of turbulent flows, *New J. Phys.* **6**, 35.

24 Musculus M., Picket l. (2009) Entrainment waves in Diesel jets, *SAE Paper* 2009-01-1335.